INTERNATIONAL JOURNAL OF LATEST TECHNOLOGY IN ENGINEERING, MANAGEMENT & APPLIED SCIENCE (IJLTEMAS)

ISSN 2278-2540 | DOI: 10.51583/IJLTEMAS | Volume XII, Issue IX, September 2023

# Integration of Rock Physics and Seismic Attributes for Reservoir Quality Assessment of 'Solid' Field, Offshore Niger Delta

**Ajisafe, Y. C., Folorunso, O. E., Omoyemi, O. V., Ogunrinde, D. E., and Towoju, V. O.**

*Department of Geology, Ekiti State University, Ado-Ekiti, Ekiti State, Nigeria*

**DOI:** https://doi.org/10.51583/IJLTEMAS.2023.12910

Received: 19 August 2023; Revised: 15 September 2023; Accepted: 20 September 2023; Published: 11 October 2023

**Abstract:** The decline in the chance of finding commercial quantity of hydrocarbon necessitated the integration of more geophysical tools in order to properly assess the reservoir quality. This study integrated rock physics and seismic attribute to assess the reservoir quality in 'Solid' field, offshore Niger Delta. The objectives of this study are to use rock physics analysis to quality check the seismic attribute results and to locate the best productive zones in the field. 3D seismic data and well log data for six wells were used for Formation evaluation, Petrophysical analysis, Structural analysis, Seismic attribute extraction. These results were then checked qualitatively using rock physics analysis. Six sand units (Sand 1, 2, 3, 4, 5 and 6) were correlated across six wells. Petrophysical analysis indicated that the reservoirs have high porosity (20.9% to 25.4%), high permeability (1897 to 2557 mD), high net-to-gross sand (84.7% to 99.0%), and low volume of shale (0.13 to 0.48). This shows that the reservoirs are of good quality. The depth structure map indicates that the reservoirs are mainly fault assisted closures. The seismic attribute extraction for the sand reservoirs shows high amplitude for Sand 1 in areas where wells have been drilled and also in some closures in Sand 2, 3 and 4 which is indicative of hydrocarbon presence. The crossplot of acoustic impedance against shear impedance of Well S5 helped to differentiate sand and shale in the reservoirs. Crossplot of acoustic impedance against Vp/Vs ratio was then used to predict the fluid type in Well S5. The crossplot of acoustic impedance against Vp/Vs ratio of Sand 2 in Well S5 and Sand 1 in Well S4 follows a regular trend with depth. The overall results portrayed that Sand 1, 2, 3 and 4 are of good quality and are oil bearing.

**Keywords:** Petrophysical parameters, Reservoir quality, Seismic attributes, Well correlation, acoustic impedance

## I. Introduction

The quality of a reservoir rock is defined by its hydrocarbon storage capacity and deliverability. The hydrocarbon storage capacity is characterized by the effective porosity and the size of the reservoir, whereas the deliverable is a function of the permeability [1]. To minimize the uncertainty of drilling for hydrocarbon in a particular area, the quality of the reservoir rock must be carefully studied and assessed. Porosity, permeability and elastic parameters are properties which determine the quality of a reservoir rock.

The field of rock physics represents the link between qualitative geological parameters and quantitative geophysical measurements [2]. The qualitative property includes elastic modulus and effective porosity while some quantitative property includes volume of shale and porosity. Rock physics laws relate porosity, mineralogy (shale content), saturation, and pore fluid properties to the elastic rock properties – elastic-wave velocity and impedance – give the connection between flow simulation and synthetic seismic imaging. Seismic attributes are defined as all of the measured, computed or implied quantities obtained from the seismic data. Seismic attributes provide a link between rock properties and seismic data [3].

The application of rock physics tools can reduce exploration risk and improve reservoir forecasting in the petroleum industry [2]. Attribute analysis of 3-D seismic data in time slice presents a great opportunity for reservoir characterization [4]. The aim of this study is to integrate rock physics and seismic attribute for assessment of reservoir rock quality in "Solid" field, Offshore Niger Delta.

## II. Geology of The Study Area

'Solid' field is an Offshore field located in Niger Delta of Nigeria (Figure 1). Niger Delta is considered to be located within nine coastal southern Nigeria states. Niger Delta is a petroleum-rich region and has now been defined official by the Nigerian government to extends over about 70,000 km$^2$ and makes up 7.5% of Nigeria's land mass [5]. The Niger Delta basin is located at the southernmost extremity of the elongated intracontinental Benue Trough of Nigeria. It is an extensional rift basin located in the Niger Delta and the Gulf of Guinea on the passive continental margin near the western coast of Nigeria [6]. The basin is separated from the Dahomey Basin by the Okitipupa basement high, and to the east it is bounded by the Cameroon volcanic line. Its northern margin transects several older (Cretaceous) tectonic elements—the Anambra basin, Abakaliki basin, Afikpo syncline, and the Calabar Flank (Figure 2a).

ISSN 2278-2540 | DOI: 10.51583/IJLTEMAS | Volume XII, Issue IX, September 2023

The evolution of the Niger delta is controlled by pre and syn-sedimentary tectonics [7, 8, 9, 10]. The tectonic framework of the continental margin along the West Coast of equatorial Africa is controlled by Cretaceous fracture zones expressed as trenches and ridges in the deep Atlantic. The fracture zone ridges (Figure 2b) subdivide the margin into individual basins, and, in Nigeria, form the boundary

faults of the Cretaceous Benue-Abakaliki trough, which cuts far into the West African shield. Three lithostratigraphic units have been recognized in the subsurface of the Niger Delta [11, 12, 13]. These are from the oldest to the youngest, the Akata, Agbada and Benin Formations (Figure 3).

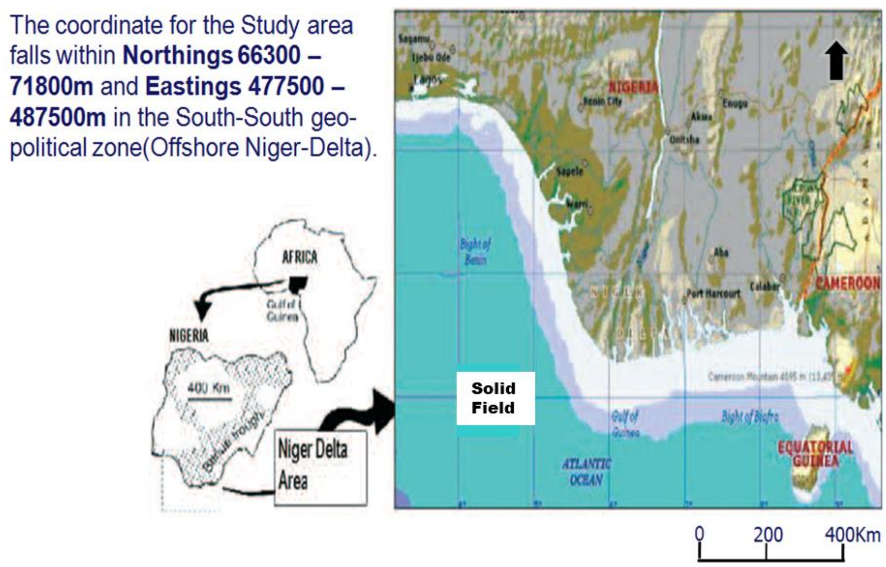


Figure 1: Image showing Location of the Study Area [14]

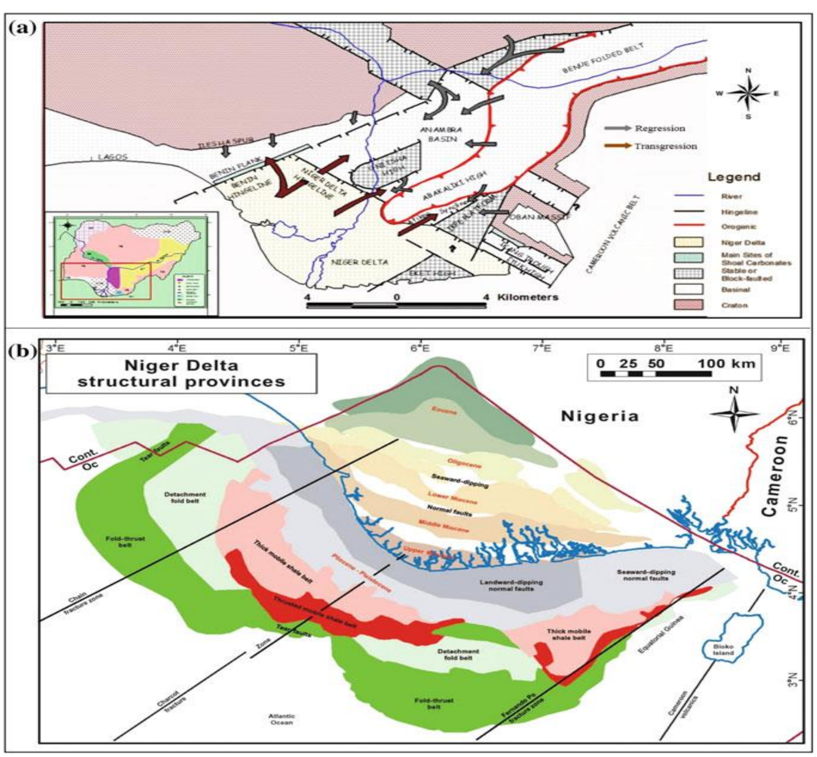


Figure 2: Tectonic Setting and Structural Elements of the Niger Delta Basin. a Tectonic Map showing the Niger Delta [15]. b Regional Structural Provinces Map of the Niger Delta showing the Fracture Zones [16].

ISSN 2278-2540 | DOI: 10.51583/IJLTEMAS | Volume XII, Issue IX, September 2023

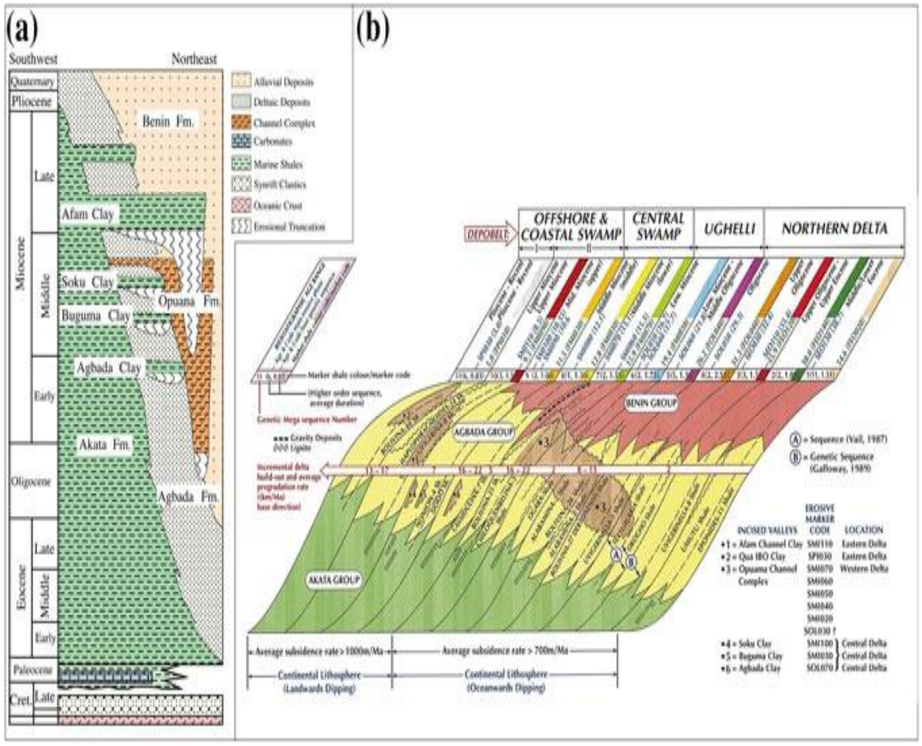


Figure 3: Stratigraphy of Niger Delta Basin. a Stratigraphic Column showing the Three Formations of the Niger Delta [17]. b Diagrammatic Representation of the Stratigraphic Evolution of the Niger Delta [18]

## III. Methodology

The data sets used for this study comprise 3D poststack time migrated seismic data (400 inlines and 220 crosslines) and well data which consist of 6 wells (4 straight and 2 deviated wells) with their wireline logs (which include gamma ray log, resistivity log, neutron log, density log and sonic log) and checkshot data.

Five interpretation steps were followed which are the Well correlation and Formation evaluation from well logs, Petrophysical Analysis, Seismic interpretation, Seismic attribute extraction and Rock physics analysis. The petrophysical parameters calculated are Gamma Ray Index ($I_{GR}$), Volume of Shale ($V_{sh}$) present in the Sand reservoir, Porosity ($\phi$), Effective Porosity (Eff. Poro), Formation water (F), Irreducible water saturation ($S_{wirr}$), Permeability (k), Water saturation ($S_w$), Hydrocarbon saturation ($S_h$) and Net to Gross sand (N/G). Structural interpretation was done by picking faults and mapping horizons based on the tops picked from the well logs. Root Mean Square (RMS) attribute, Maximum Amplitude attribute and Average Energy attributes were extracted from the reservoirs picked. Rock physics was used to check the lithology and fluid type present in the reservoirs. The cross plot of the Acoustic Impedance (AI) vs Shear Impedance (SI) was used to check the lithology present in the wells and the cross plot AI and Vp/Vs ratio was used to check the fluid type present.

## IV. Results And Discussion

### 4.1 Well Correlation and Formation Evaluation from Logs

Six sand packages were picked across all the wells (Figure 3). The correlation between well S3 and well S6 which is a correlation in the dip direction shows that the lithologies are not horizontally laid but have been tilted, dipping towards the south. This can also be seen in the correlation of wellS4 and Well S3. The distance between well S3 and well S6 is 129 meters and the throw is 800ft (264 meters) south. The dip angle is calculated to be 62.12$^o$.

From the log analysis, Sand 1, Sand 2, and Sand 4 showed high resistivity and crossover of Neutron and Density log (Figure 4). This signature is typical of a hydrocarbon bearing reservoir. The crossover of the neutron and density cross plot did not show any typical balloon shape, hence it can be said that the reservoir is oil bearing and non-gas bearing.

Most of the sands show crossover of the neutron density cross plot but low resistivity. The low resistivity signature indicate that hydrocarbon is absent in the well. The high neutron means that there more hydrogen atom in the reservoir.

ISSN 2278-2540 | DOI: 10.51583/IJLTEMAS | Volume XII, Issue IX, September 2023

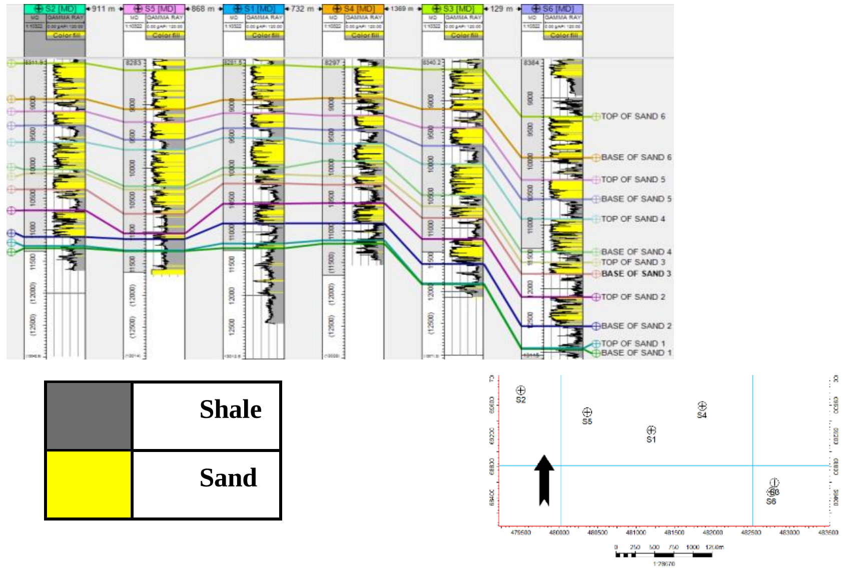


Figure 3: Lithostratigraphy correlation of the Six Wells

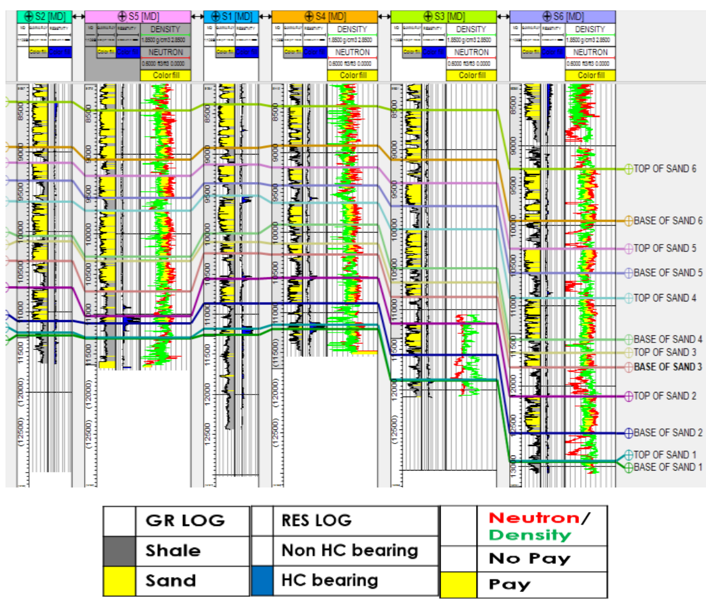


Figure 4: Formation evaluation of the Wells from Logs

### 4.2 Petrophysical Analysis of the Reservoirs

The petrophysical parameters for the wells were extracted and calculated. This is shown in Table 1. The parameters were used to know the reservoir properties and fluid content of the reservoirs.

Table 1. Petrophysical Parameters for the Reservoirs

| Reservoir | Thickness (ft) | Por. Eff. | $S_w$ | $S_h$ | $V_{shale}$ | K | N/G |
|---|---|---|---|---|---|---|---|
| Sand 6 | 636.500 | 0.216 | 0.903 | 0.097 | 0.498 | 1879.235 | 0.847 |
| Sand 5 | 290.500 | 0.254 | 0.985 | 0.015 | 0.484 | 2039.663 | 0.990 |
| Sand 4 | 479.667 | 0.235 | 0.689 | 0.311 | 0.315 | 2557.167 | 0.927 |

ISSN 2278-2540 | DOI: 10.51583/IJLTEMAS | Volume XII, Issue IX, September 2023

| | | | | | | | |
|---|---|---|---|---|---|---|---|
| Sand 3 | 247.333 | 0.219 | 0.712 | 0.288 | 0.361 | 2471.952 | 0.879 |
| Sand 2 | 317.000 | 0.209 | 0.615 | 0.385 | 0.274 | 2032.749 | 0.857 |
| Sand 1 | 67.667 | 0.211 | 0.236 | 0.764 | 0.138 | 2229.337 | 0.835 |

All the sand reservoirs are thick except sand 1 whose thickness is considerably small compared with other reservoirs. The porosity of the sand reservoirs were high enough for a quality reservoir rock. The porosity of a good reservoir rock ranges from 10% to 30% [19]. The average porosity of all the sand reservoirs falls between this range. The volume of shale of the sands is low for Sand 1, Sand 2, Sand 3 and Sand 4 and comparatively lower to the volume of shale in Sand 5 and Sand 6. The volume of shale increases as we move upward from sand 1 to sand 6. Volume of shale is a function of productability of a reservoir therefore, Sand 1, 2, 3, 4, having lower value of volume of shale will be more productive than Sand 5 and Sand 6. The permeability of the sand reservoirs is also greater than 250mD. A good reservoir rock is said to have permeability greater than 250mD[19].

All the reservoirs have Net to Gross sand which is high, greater than 83%. This indicates that the quantity of sand present in the reservoirs picked is high. Sand is known to be the reservoir in Niger Delta which is the study area. All the aforementioned parameters show that the reservoirs are of good quality and all have the potential to hold hydrocarbon. One important petrophysical parameters which is used to know the fluid type in the reservoir is the water saturation parameter. As a reservoir can only be hydrocarbon bearing or water bearing, the water saturation shows the percentage of water in the reservoir. Water saturation is related to hydrocarbon saturation with the formula.

Therefore, if the water saturation is high, the quantity of probable hydrocarbon in the reservoir will be low. Sand 1 has the highest percentage of hydrocarbon saturation which is 76.4% of the total fluid present in the reservoir. Sand 2 has 38.6%, Sand 3 has 28.8%, Sand 4 has 31.1%, Sand 5 has 1.5% and Sand 6 has 9.7% of hydrocarbon.

Comparing the fraction of hydrocarbon present with the thickness of the reservoirs, Sand 1, 2, 3, and 4 are likely to be of economic value for prospect. These reservoirs are mapped on seismic section and attributes are generated.

### 4.3 Structural Interpretation

The synthetic seismogram generated for Well S5 (Figure 5) shows a good match indicating that the well is properly placed on the seismic section.

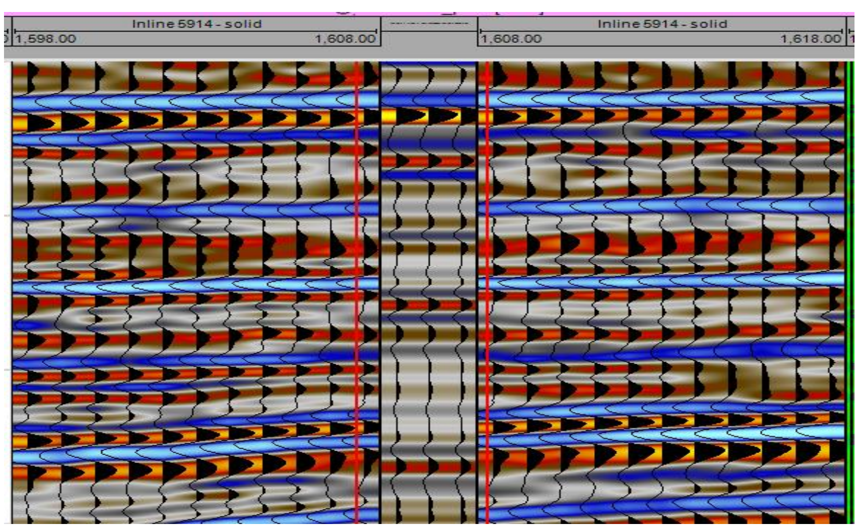


Figure 5: Well S4 Synthetics Seismogram

Sand 1, 2, 3, 4 and 6 were mapped and the horizons were converted to time structural map. The time structural map was then converted to a depth map depth structural map. The faults were also picked. 7 faults, 2 regional faults and 5 local faults cut across the reservoirs and were labeled F1, F2, F3, F4, F5, F6 and F7 (Figure 6a, 6b)

The picking of Sand 1, 2, 3, and 4 reservoirs is based on their hydrocarbon saturation ($S_h$) which has been discussed above to be high. Sand 6 was picked so as to be used for control study of the reservoirs which are earlier said to be hydrocarbon bearing. The colour calibration of the map ranges

ISSN 2278-2540 | DOI: 10.51583/IJLTEMAS | Volume XII, Issue IX, September 2023

from purple which shows area of higher time to red which shows areas of lower time. This can be interpreted in terms of the stratigraphy, dip and anticlinal structure of the top of the reservoirs.

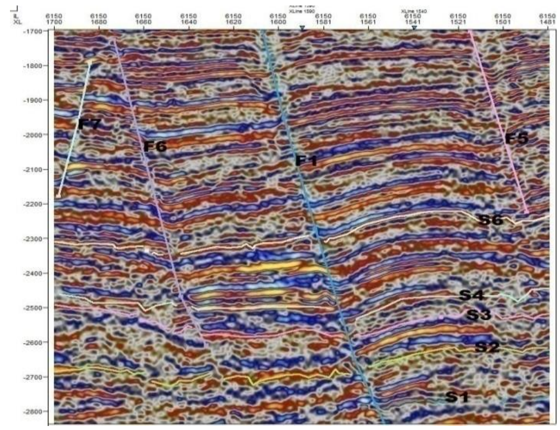

Figure 6a: Seismic section showing fault F1, F5, F6, F7 and all horizons.

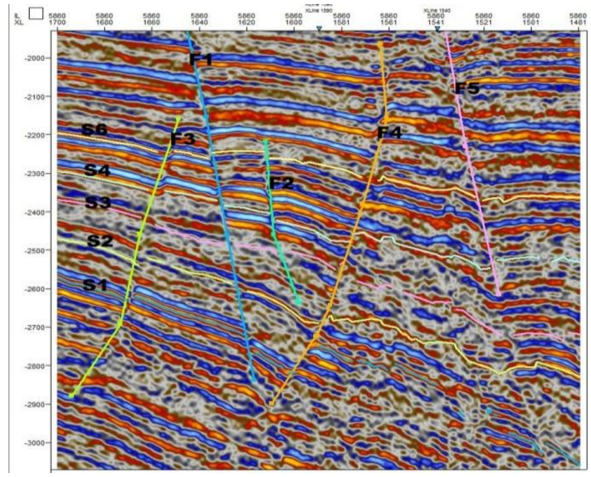

Figure 6b: Seismic section showing fault F1, F2, F3, F4, F5 and all horizons

There are two Leads, three Prospects and a discovery in the depth map of sand 1 (Figure7a). The leads are labeled L1 and L2, the prospects are labeled P1, P2, P3 and the discoveries are labeled D. Closure P1, P2, and P3 terminates against fault F3, F5 and F5 respectively. Therefore, they are regarded as 3 way closures.

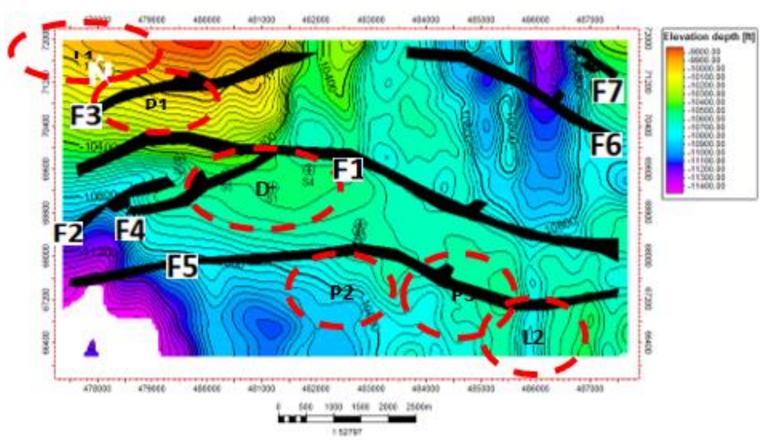

Figure 7a: Depth structure map of sand 1

INTERNATIONAL JOURNAL OF LATEST TECHNOLOGY IN ENGINEERING, MANAGEMENT & APPLIED SCIENCE (IJLTEMAS)

ISSN 2278-2540 | DOI: 10.51583/IJLTEMAS | Volume XII, Issue IX, September 2023

In the depth map of sand 2, there are one lead, two prospects and one discovery (Figure 7b). Prospect P1 and P3 terminate against fault F3 and F5 respectively therefore forming a typical 3-way closure.

Sand 3 have seven anticlinal structure which include one lead, four prospects and one discovery (Figure 7c). At this depth, prospect P4 is a 4-wayclosure while prospect P1 and P3 are 3-way closure closing against fault F3, F1 and F5 respectively. Prospect P5 is a typical 2-way closure closing against fault F1 and F2.

There are eight closures in sand 4 which include three leads, four prospects and one discovery. Prospect P4 remains a 4-way closure at this depth and prospect P1 and P5 are still 3-way closure closing against fault F3, and F5 respectively (Figure 7d). A new prospect P6 emerged at this depth which is a 3-way closure closing against fault F6.

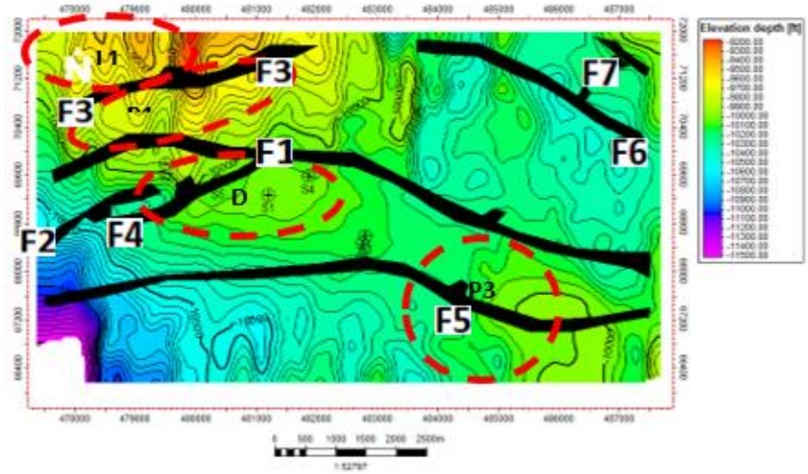


Figure 7b: Depth structure map of sand 2

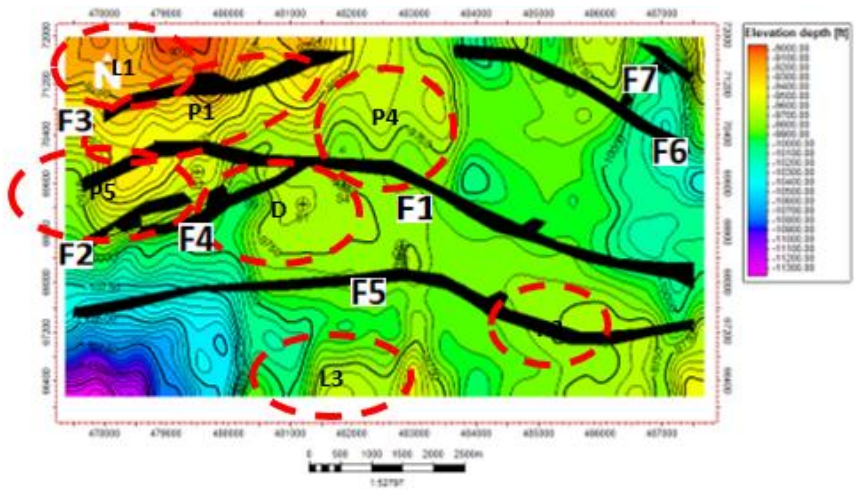


Figure 7c: Depth structure map of sand 3

Sand 6 have seven which include three leads, four prospects and one discovery (Figure 7e). All the prospects and leads at this depth coincides with prospects which have been delineated in other reservoirs.

**4.4 Seismic Attribute Analysis**

From the petrophysical parameters and the structure maps generated, sand 1, 2, 3 and 4 still have high probability of containing hydrocarbon because they have high hydrocarbon saturation and closures that can hold hydrocarbon. Direct hydrocarbon indicators (DHIs) which are the RMS, Maximum Amplitude and Average energy amplitude were extracted. Closures with high attributes are probable hydrocarbon bearing zone. It should be noted that the attributes were extracted based on the top of the reservoirs and not the reservoir intervals.

ISSN 2278-2540 | DOI: 10.51583/IJLTEMAS | Volume XII, Issue IX, September 2023

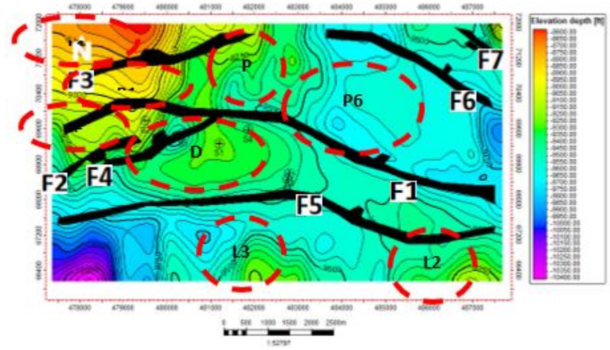


Figure 7d: Depth structure map of sand 4

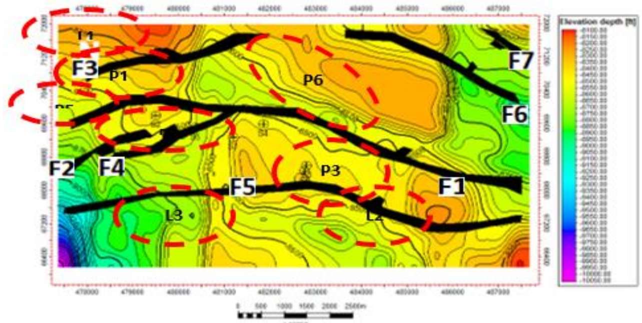


Figure 7e: Depth structure map of sand 6

The attribute maps extracted for sand 1 show high amplitude values at the discovery which is indicative that the wells drilled in the area are producing hydrocarbon (Figure 8a, 8b, 8c). This is confirming that areas with high attributes are probable hydrocarbon bearing zone.

Some part of Prospect P1 in Sand 2 has high amplitude value and therefore likely to contain hydrocarbon (Figure 8d, 8e, 8f). Attributes extracted for sand 3 shows area of high attribute value at prospect P4 and also most likely to be hydrocarbon bearing (Figure 8g, 8h, 8i).

Sand 4 have high amplitude value at prospect P6. Prospect P6 is a 3-way closure which terminate against well Fault F6 (Figure 8j, 8k, 8l). Sand 6, though have well defined closures, have no area of high attributes value (Figure 8m, 8n, 8o). This confirms that well S6 is non hydrocarbon bearing.

Seismic attribute has therefore showed prospect P1 in Sand 2, P4 in sand 3 and P4 in Sand 4 to be the best prospects. Sand 6 have no area of high amplitude value and therefore confirming that it is a water bearing reservoir as well log and petrophysical analysis as earlier proved. Rock physics crossplots are used to know the fluid type in these reservoirs.

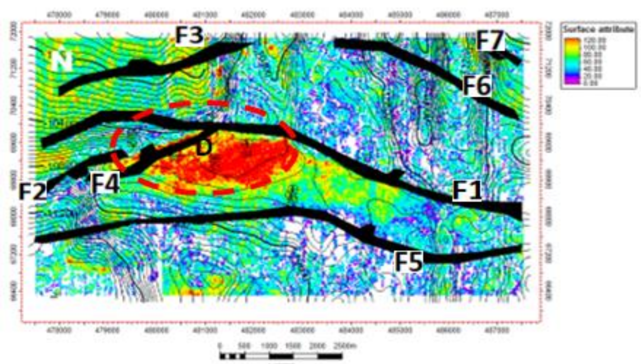


Figure 8a: RMS Attribute map of sand 1

ISSN 2278-2540 | DOI: 10.51583/IJLTEMAS | Volume XII, Issue IX, September 2023

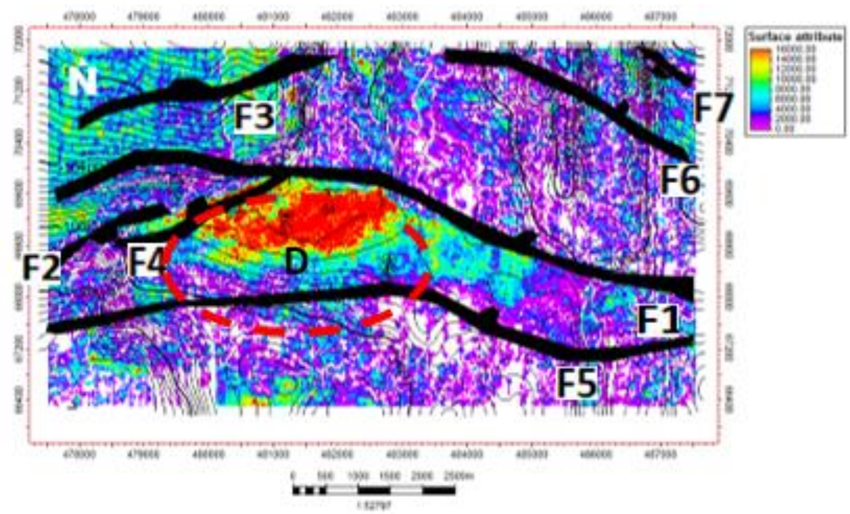


Figure 8b: Average Energy Attribute map of sand 1

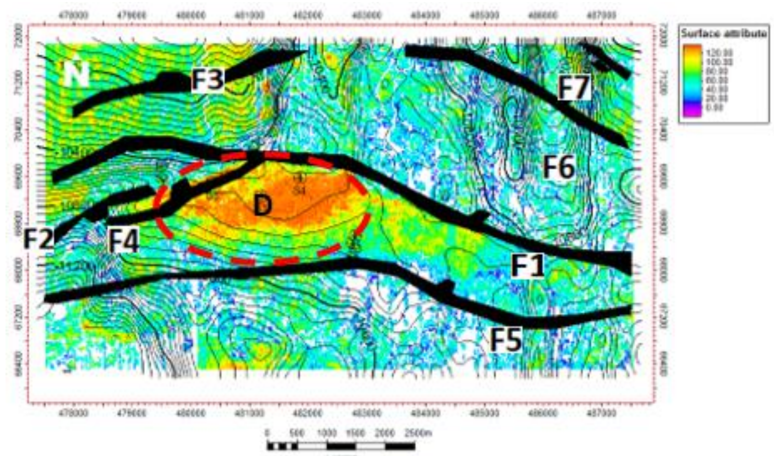


Figure 8c: Maximum Amplitude Attribute map of sand 1

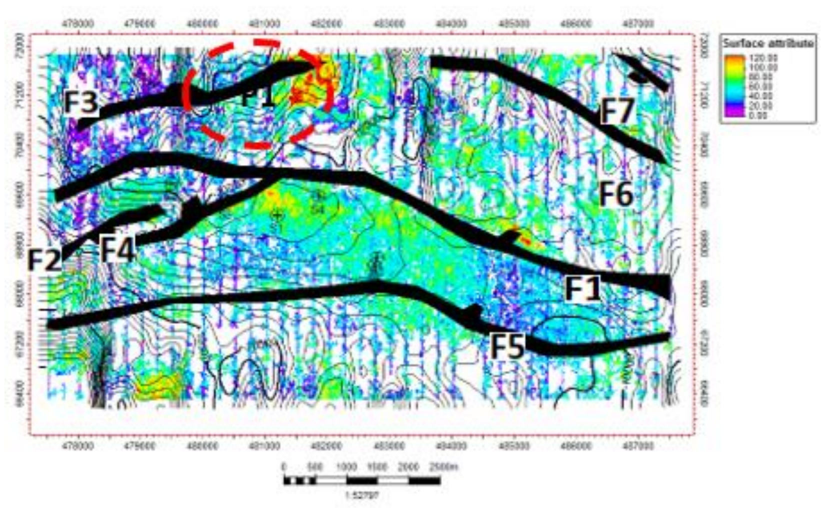


Figure 8d: RMS Attribute map of sand 2

INTERNATIONAL JOURNAL OF LATEST TECHNOLOGY IN ENGINEERING, MANAGEMENT & APPLIED SCIENCE (IJLTEMAS)
ISSN 2278-2540 | DOI: 10.51583/IJLTEMAS | Volume XII, Issue IX, September 2023

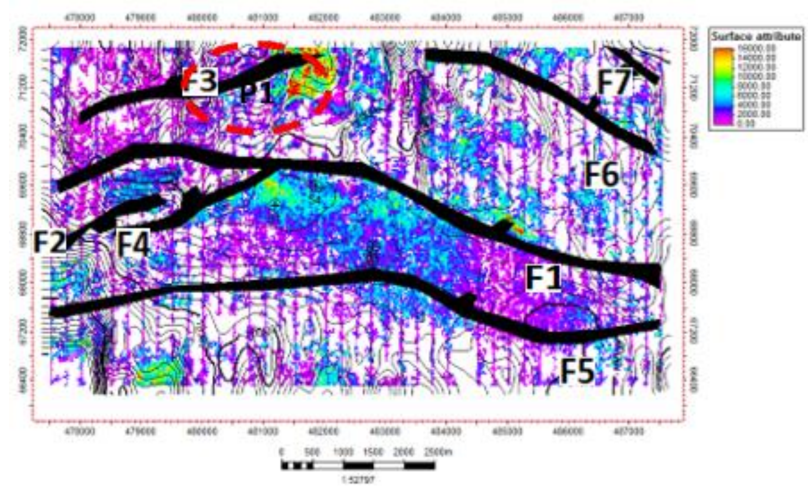


Figure 8e: Average Energy Attribute map of sand 2

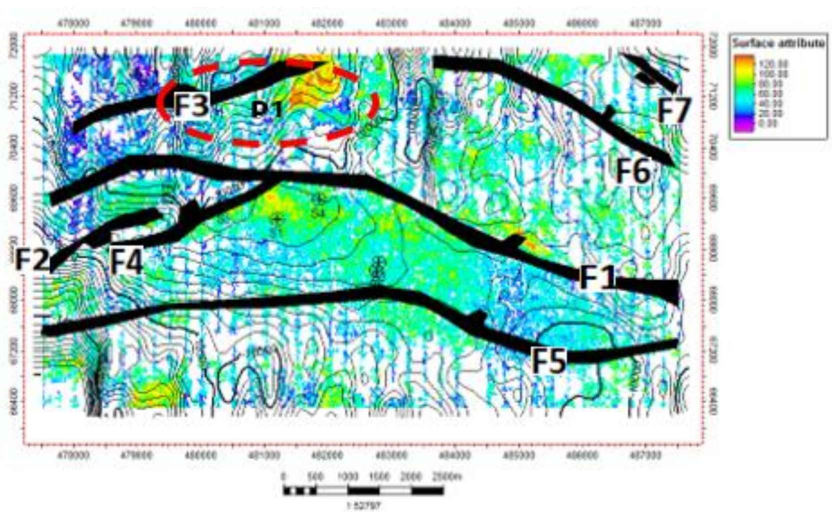


Figure 8f: Maximum Amplitude Attribute map of sand 2

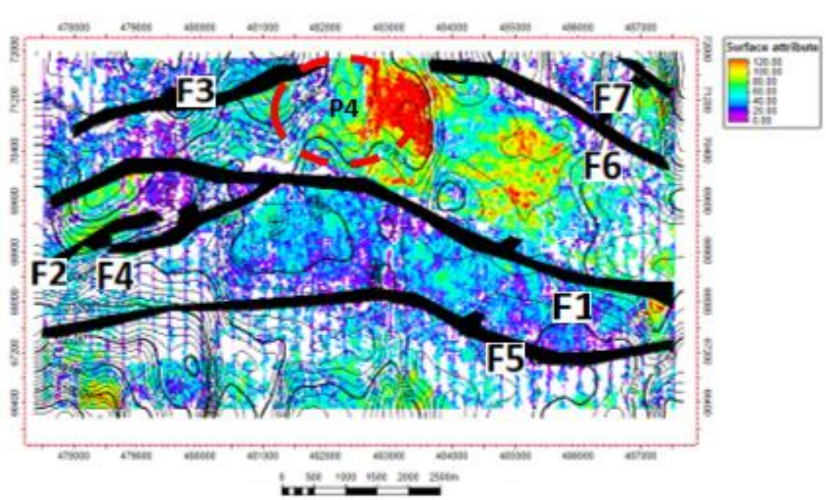


Figure 8g: RMS Attribute map of sand 3

ISSN 2278-2540 | DOI: 10.51583/IJLTEMAS | Volume XII, Issue IX, September 2023

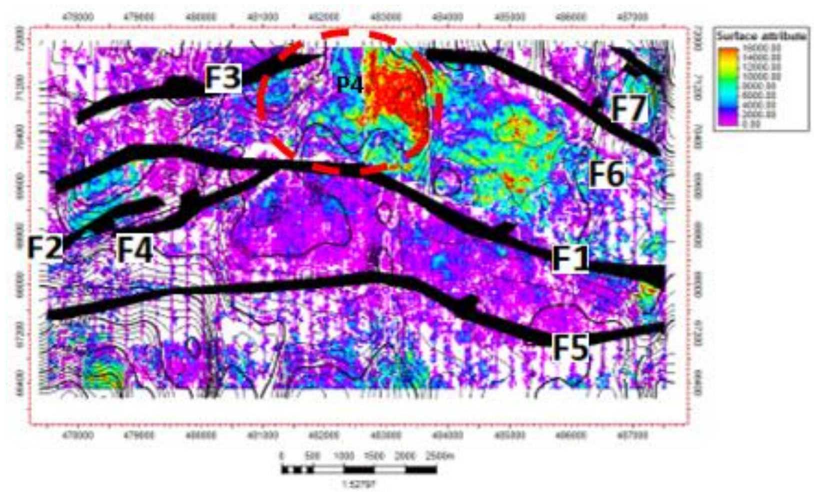


Figure 8h: Average Energy Attribute map of sand 3

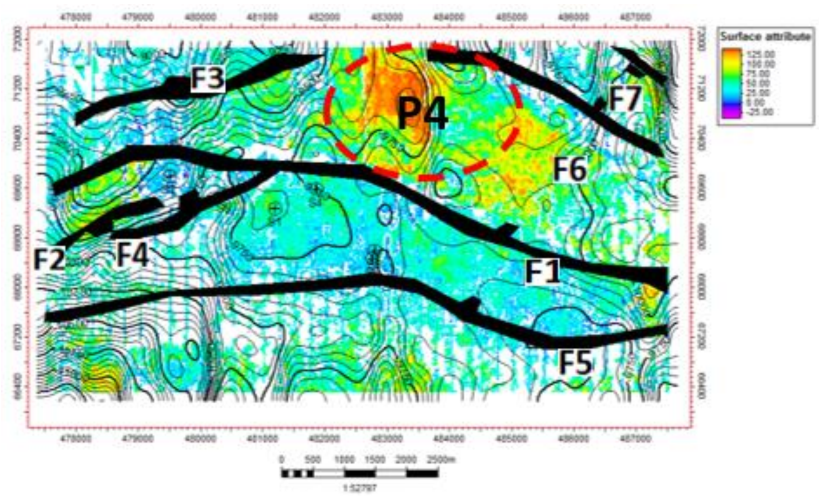


Figure 8i: Maximum Amplitude Attribute map of sand 3

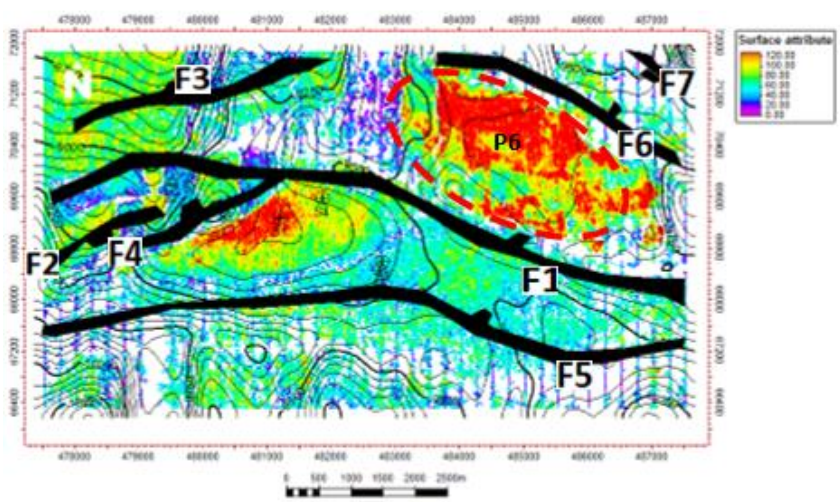


Figure 8j: RMS Attribute map of sand 4

INTERNATIONAL JOURNAL OF LATEST TECHNOLOGY IN ENGINEERING, MANAGEMENT & APPLIED SCIENCE (IJLTEMAS)

ISSN 2278-2540 | DOI: 10.51583/IJLTEMAS | Volume XII, Issue IX, September 2023

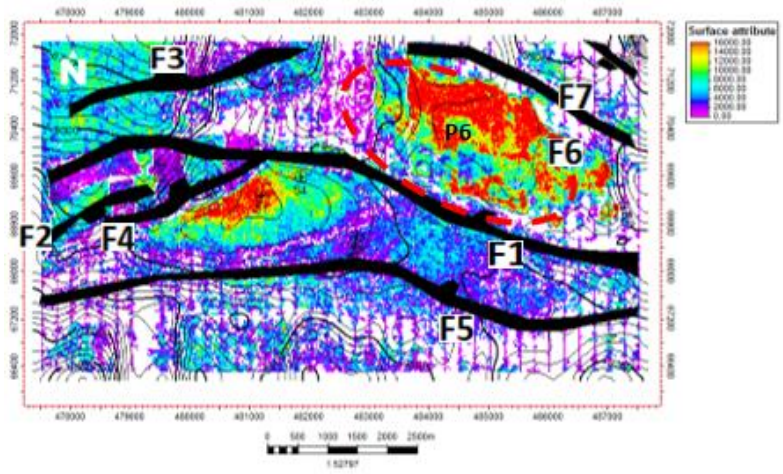


Figure 8k: Average Energy Attribute map of sand 4

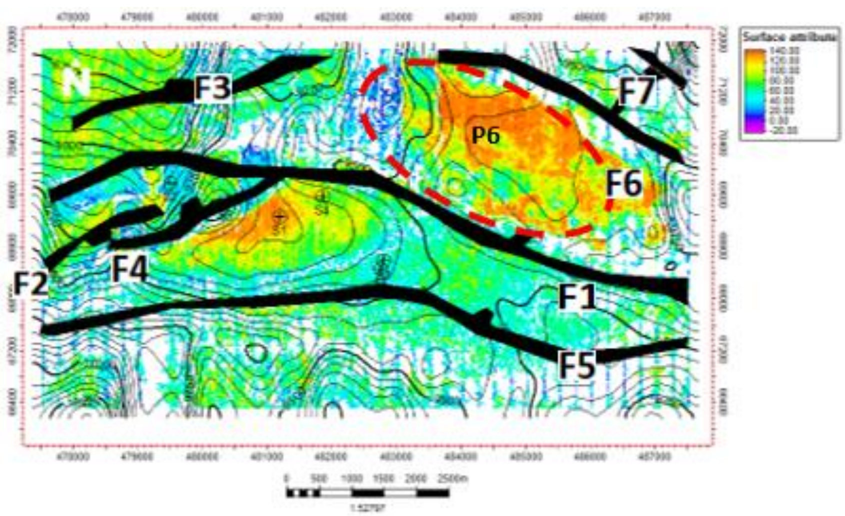


Figure 8l: Maximum Amplitude Attribute map of sand 4

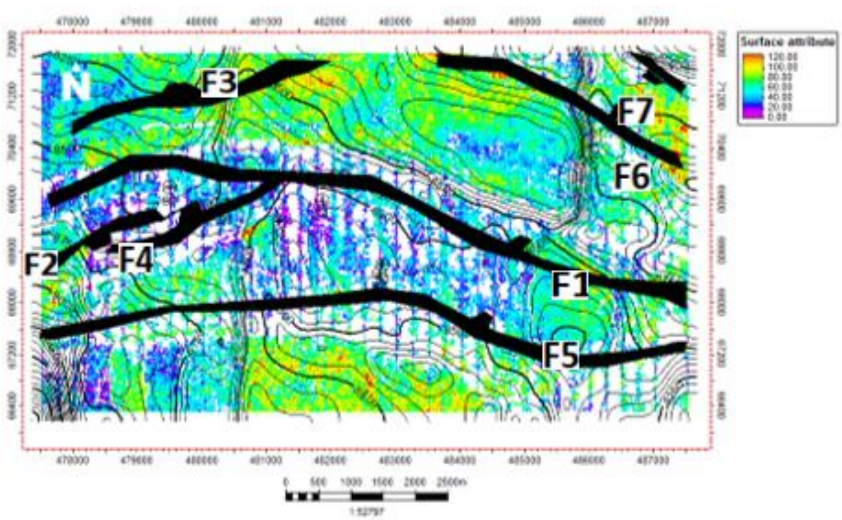


Figure 8m: RMS Attribute map of sand 6

ISSN 2278-2540 | DOI: 10.51583/IJLTEMAS | Volume XII, Issue IX, September 2023

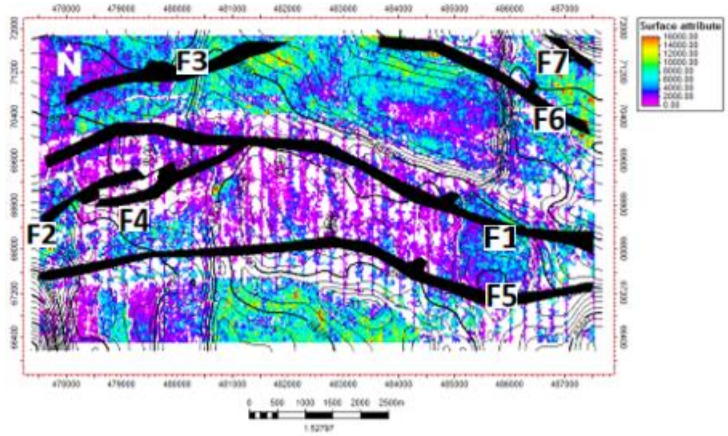


Figure 8n: Average Attribute map of sand 6

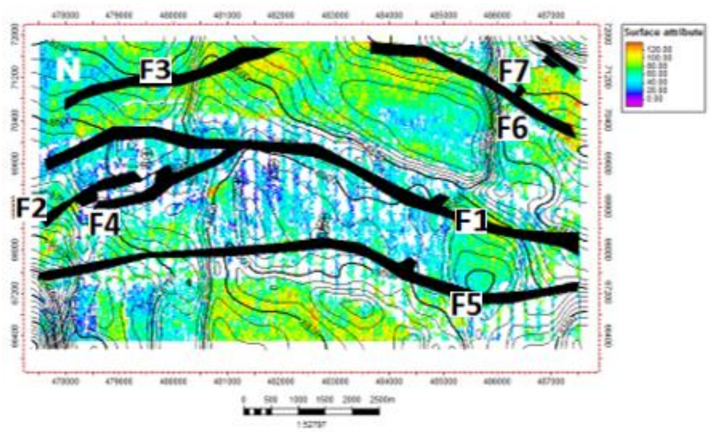


Figure 8o: Maximum Amplitude Attribute map of sand 6

### 4.5 Rock Physics

Having confirmed, using well logs, petrophysical parameters, structural analysis and seismic attributes, the area of probable hydrocarbon presence, elastic parameters from rock physics are also cross plotted to know more about the reservoir quality and fluid type present.

The cross plot of Acoustic Impedance (AI) and Shear Impedance (SI) of well S5 colour coded with facies (Figure 9a) shows a distinction between the sand and the shale present in the reservoir. The black line shows the sand trend while the red line shows the shale trend. This difference is due to the porosity and permeability of sand which is higher than that of shale. Sand therefore will contain more fluid than shale and fluid presence account for these changes in the compressional velocity and shear velocity of the seismic wave and therefore resulting to change in the acoustic impedance and shear impedance of the two different lithologies.

The distinction in the facies displayed by the crossplot of AI and SI is indicative that rock physics can be used for lithology discrimination in a reservoir. This can help in the understanding of the lithologies of a reservoir beyond the well cover and to know the quantity of sand in a reservoir.

The crossplot of acoustic impedance and Vp/Vs ratio for well S5 colour coded with facies (Figure 9b) shows a nonlinear trend of sand and shale which is also distinctive. This crossplot works of lithology discrimination as the crossplot of AI vs SI. The difference is that AI and SI crossplot gives a linear trend for litholgies while corssplot of AI vs Vp/Vs gives a nonlinear trend. Another minor sand trend is seen below the shale. The upper sand trends are the sands of the Benin Formation which is brine filled while the lower thing sand trend are the sand of the Agbada Formation which is our concern in this study.

The crossplot of AI vs Vp/Vs is also colour coded with density, resistivity, net to gross sand and water saturation. The result of the crossplot is then used to generate a template for fluid discrimination of the well.

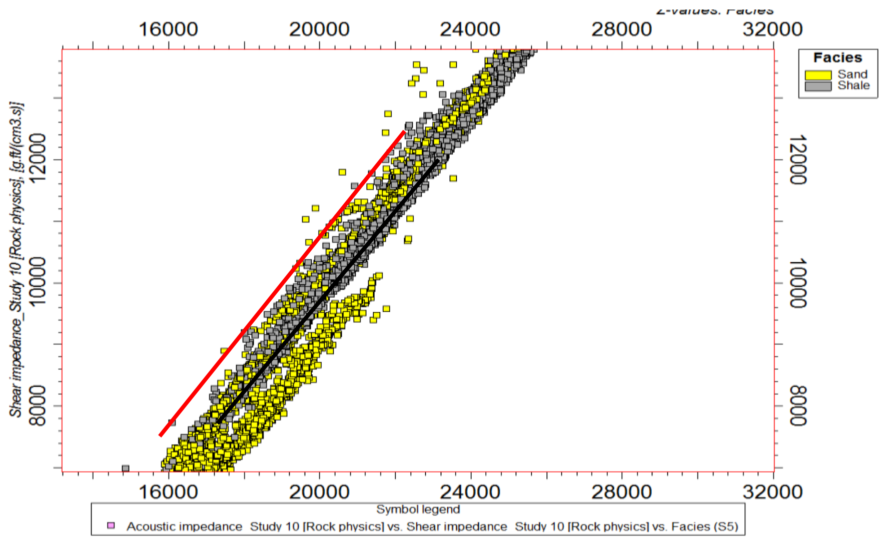


Figure 9a: Rock physics crossplot of AI vs SI vs Facies for well S5

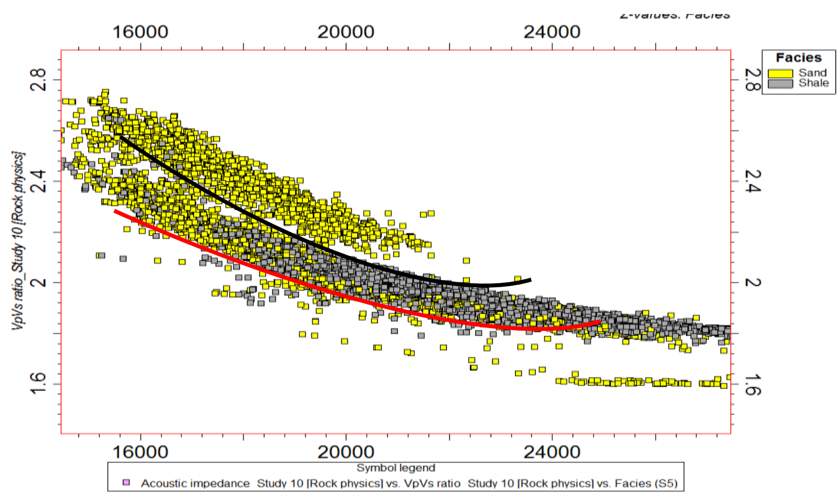


Figure 9b: Rock physics crossplot of AI vs Vp/Vs vs facies for well 5

The crossplot of AI vs Vp/Vs colour coded with density (Figure 9c) shows a density difference in the well. The density of sand labeled ‘I’ in black circle is high which is indicative of a non-hydrocarbon bearing sand. This is because a hydrocarbon bearing sand is typical of low density. It is therefore justified that the sand belongs to the Benin Formation. The shale trend with red colour line is also having high density which is also characteristic of typical shale and there is low density reading below the shale which is probable hydrocarbon bearing sands whose tend is shown in green line.

The crossplot when colour coded with net to gross (Figure 9d) the red dots are areas of high net to gross while the purple dots show areas of low net to gross. This is confirming the presence of thin trend of sand below the shale. The trend is marked with green line. The area of green trend line slightly below the shale is having low density and high net to gross therefore characteristics of hydrocarbon.

The crossplot is then colour coded with resistivity (Figure 9e) and water saturation (Figure 9f). The red coloured dots shows area of high resistivity and the red coloured dots also shows areas of low water saturation. These two properties – high resistivity and low water saturation – is typical of hydrocarbon bearing reservoir. This conforms to the crossplots shown earlier to discriminate lithology. The probable hydrocarbon bearing sand is circled green, the brine sand is circles black and the shale is circled red.

From the crossplots shown, it is observed that the hydrocarbon bearing sand follows a regular trend and no anomaly. This therefore shows that there are no gases in the reservoirs. Gas is known to have a different AI and Vp/Vs ratio different from that of hydrocarbon bearing sand. It is therefore concluded that there are no gasses in the field.

ISSN 2278-2540 | DOI: 10.51583/IJLTEMAS | Volume XII, Issue IX, September 2023

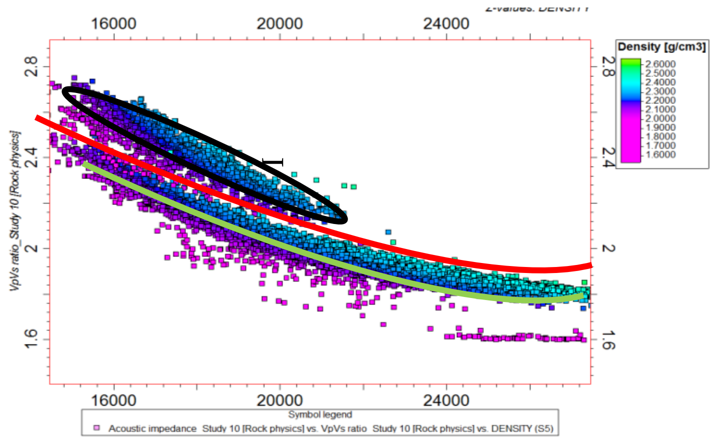


Figure 9c: Rock physics crossplot of AI vs Vp/Vs ratio Vs density for well S5

The crossplot of AI against Vp/Vs ratio of the sand 4 colour coded with resistivity (Figure 10) also shows that the hydrocarbon bearing zones follows a regular trend

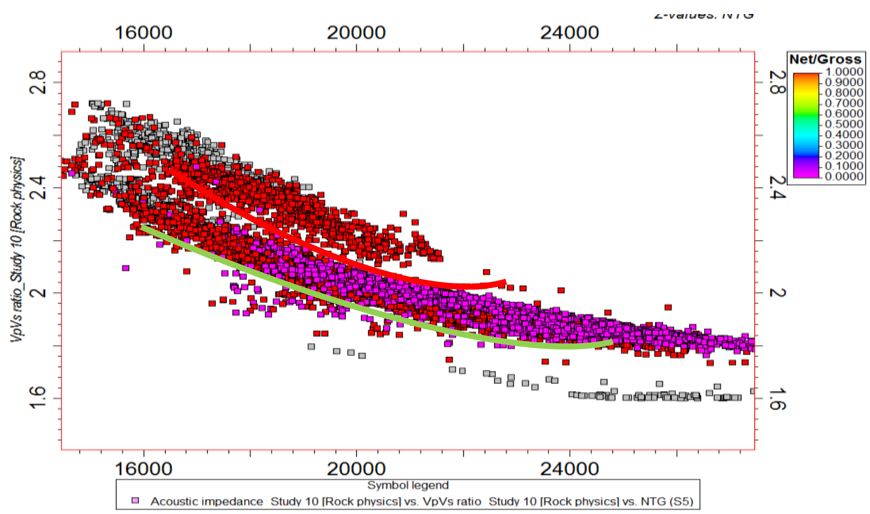


Figure 9d: Rock physics crossplot of AI vs Vp/Vs ratio Vs net to gross for well S5

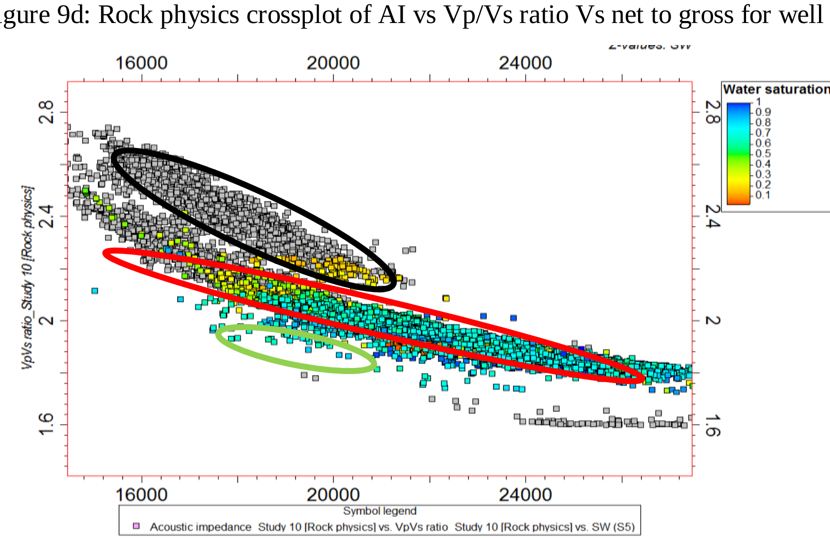


Figure 9e: Rock physics crossplot of AI vs Vp/Vs ratio vs Resistivity of Sand 5.

ISSN 2278-2540 | DOI: 10.51583/IJLTEMAS | Volume XII, Issue IX, September 2023

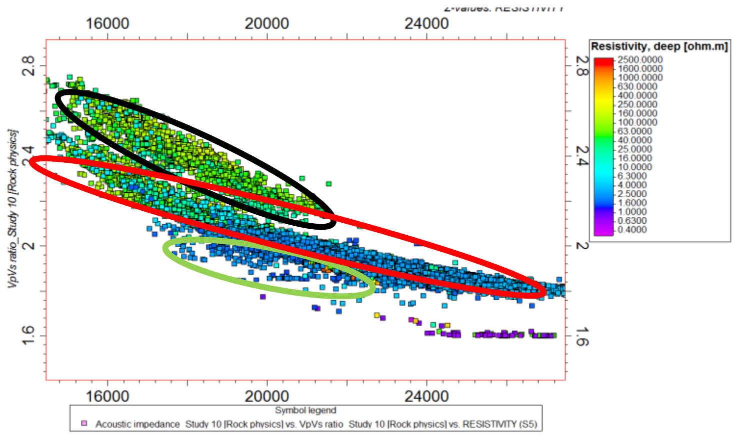


Figure 9f: Rock physics crossplot of AI vs Vp/Vs ratio vs Sw of Sand 5

and therefore non gas bearing. The crossplot of AI against Vp/Vs ratio of hydrocarbon bearing sands colour coded with water saturation (Figure 11) in well S4 and well S5 are plotted together. There is also a regular trend of the hydrocarbon bearing sands. It is therefore confirmed that the sands in the field is only oil bearing and non-gas bearing.

The crossplot are used to build a rock physics template (Figure 12) for lithology and fluid discrimination in a well. The first three crossplots (Figure 9a, b, c) are used for lithology identification while the last three crossplots (Figure 9d, e, f) are used for fluid discrimination.

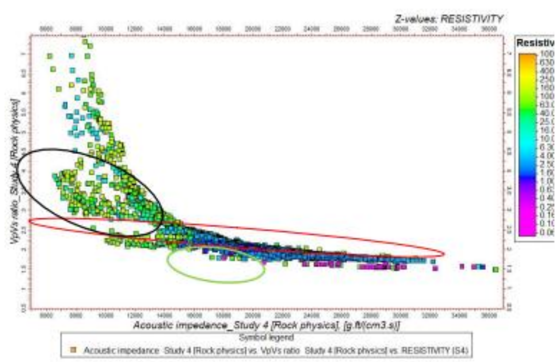


Figure 10: Generated rock physics template on Sand 4 AI vs Vp/Vs vs Resistivity

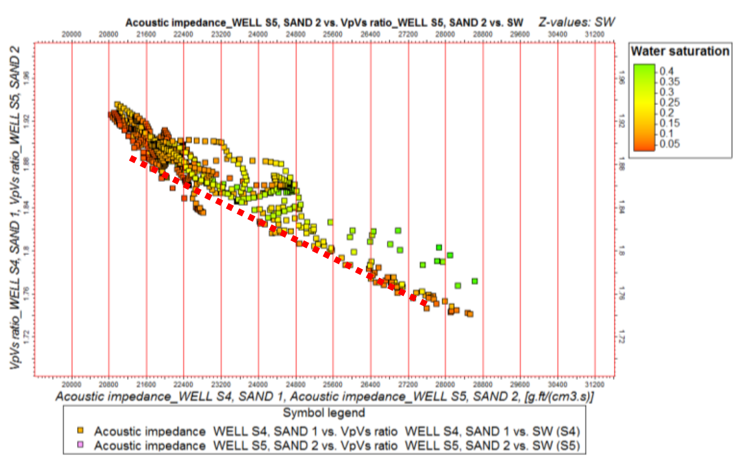


Figure 11: Cross plot of sand 1 and Sand 2 in well S4 and S5 respectively

ISSN 2278-2540 | DOI: 10.51583/IJLTEMAS | Volume XII, Issue IX, September 2023

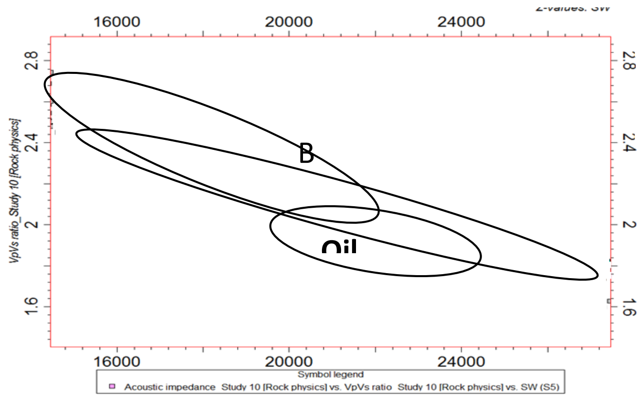


Figure 12: Generated rock physics template

## V. Conclusions

The integration of rock physics and seismic attributes has helped to better understand the reservoir quality in "Solid" field. The study has been able to delineate from well log analysis that Sand 1, 2 and 4 are hydrocarbon bearing and that Sand 1, 2, 3, and 4, from petrophysical parameter calculation, have high porosity, permeability and hydrocarbon saturation. Structural study of the Sand reservoirs shows that all the reservoirs have closures which can hold hydrocarbon. Two way, three way and four way closures can be seen on the maps generated for the reservoirs. The trapping style in the area is majorly fault dependent anticlinal closures.

Seismic attributes confirm prospect P1, P4 and P6 in Sand 2, Sand 3 and Sand 4 respectively to be hydrocarbon bearing.The seismic structural interpretation, attributes and petrophysical analysis were then checked qualitatively using rock physics analysis. The crossplot acoustic impedance against shear impedance of Well S5 helped to differentiate the sand and shale in the reservoirs therefore allowing us to predict the quantity of sand in the reservoir. The crossplot of acoustic impedance against Vp/Vs ratio was then used to predict the fluid type in Well S5. The crossplot of acoustic impedance against Vp/Vs ration of Sand 2 in Well S5 and Sand 1 in Well S4 follows a regular trend with depth therefore, it is concluded that the reservoirs are oil bearing. The overall results portrayed that structural trap, the reservoir characteristics are useful impute to the volumetric analysis to evaluate prospect of the reservoir area.

## References


1. McBride, E. F. (1984). Compaction in sandstones—influence on reservoir quality: AAPG Bulletin, v. 68, p. 505
2. Avseth, P. and Bjørlykke K. (2010). Petroleum Geoscience: From Sedimentary Environments to Rock Physics. Springer-Verlag Berlin Heidelberg, 47-49.
3. Ajisafe, Y. C. and Ako, B. D. (2013). 3D Seismic Attributes for Reservoir Characterization of "Y" Field, Niger Delta, Nigeria. International Journals of Geology and Geophysics, 1(2): 23-31.
4. Vetrici, D. G. and Stewart, R. R. (1996). 3-D seismic attributes. CREWES Research Report, 8: 45 – 75.
5. CRS Report for Congress, Nigeria: Current Issues. Updated 30, January 2008.Adesida, A., & Ehirim, B. O. (1988). Cenozoic Niger Delta: A guide to its lithosedimentary analysis. SPDC Exploration note 88.002 (Ref: on-shore wells) 1–10.
6. Tuttle, M., Charpentier, R. and Brownfield, M. (2015). The Niger Delta Petroleum System: Niger Delta Province, Nigeria, Cameroon, and Equatorial Guinea, Africa. United States Geologic Survey. United States Geologic Survey Bulletin, 5: 34-45.
7. Evamy, B. D., Haremboure, J., Kamerling, P., Knaap, W. A., Molloy, F. A. and Rowlands, P. H. (1978). Hydrocarbon habitat of Tertiary Niger Delta. American Association of Petroleum Geologists Bulletin, 62: 1–39.
8. Ejedawe, J. E. (1981). Patterns of incidence of oil reserves in Niger delta basin. American Association of Petroleum Geologists Bulletin, 65: 1574–1585.
9. Knox, G. J. and Omatsola, E. M. (1987). Development of the Cenozoic Niger delta in terms of the "Escalator Regression" model and impact on hydrocarbon distribution. In Proceedings of the KNGMG Symposium on Coastal Lowlands, Geology and Geotechnology, 181–202.
10. Stacher, P. (1995). Present Understanding of the Niger Delta hydrocarbon habitat. In Oti M. N. and G. Postma (Eds.), Geology of Deltas, 257–267.

ISSN 2278-2540 | DOI: 10.51583/IJLTEMAS | Volume XII, Issue IX, September 2023


11. Short, K. C. and Stauble, A. J. (1967). Outline of geology of Niger Delta. American Association of Petroleum Geologists Bulletin, 51, 761–779.
12. Frankl, E. J. and Cordy, E. A. (1967). The Niger Delta oil province: Recent developments onshore and offshore. In Proceedings of the Seventh world petroleum congress, 2: 195–209.
13. Avbovbo, A. A. (1978). Tertiary lithostratigraphy of Niger Delta. American Association of Petroleum Geologists Bulletin, 5: 96–200.
14. Owoyemi, A. O. and Willis, B. J. (2006). Depositional patterns across syndepositional normal faults, Niger Delta, Nigeria. J Sediment Res 76(1-2): 346-363.
15. Kogbe C. A. (1989). The Cretaceous Paleocene sediments of Southern Nigeria. In: Kogbe, C. A. (ed) Geology of Nigeria. Rock View Ltd., Jos, pp 320-325.
16. Wiener, R. W., Mann, M. G., Angelich, M. T. and Molyneux, J. B. (2010). Mobile shale in the Niger Delta: Characteristics, structure, and evolution. In L. Wood (Ed.), Shale tectonics American Association of Petroleum Geologists Memoir, 93: 145–161.
17. Lawrence, S. R., Munday, S. and Bray, R. (2002). Regional geologh and geophysics of the eastern Gulf of Guinea (Niger Delta to Rio Muni). Leading Edge 21:112-117.
18. Reijers, T. R. A. (2011). Stratigraphy and sedimentology of the Niger Delta. Andea Geol 17 (3):133-162.
19. Adeoti, L., Adeleye, K. O., Itsemode, A. and Bello, M. A. (2014). Fluid prediction using AVO analysis and forward modelling of deep reservoirs in Faith Field, Niger Delta, Nigeria, Arabian Journal of Geosciences, 10:1-20.